




Cite this: *RSC Adv.*, 2021, 11, 17222

# Pressure-induced stability and polymeric nitrogen in alkaline earth metal N-rich nitrides ( $\text{XN}_6$ , $\text{X} = \text{Ca}$ , $\text{Sr}$ and $\text{Ba}$ ): a first-principles study†

Zhipeng Liu, Shuli Wei, \* Yanhui Guo, Haiyang Sun, Hao Sun, Qiang Chang and Yuping Sun \*

Multi-nitrogen or polynitrogen compounds can be used as potential high energy-density materials, so they have attracted great attention. Nitrogen can exist in alkaline earth metal nitrogen-rich (N-rich) compounds in the form of single or double bonds. In recent years, to explore N-rich compounds which are stable and easy to synthesize has become a new research direction. The N-rich compounds  $\text{XN}_6$  ( $\text{X} = \text{Ca}$ ,  $\text{Sr}$  and  $\text{Ba}$ ) have been reported under normal pressure. In order to find other stable crystal structures, we have performed  $\text{XN}_6$  ( $\text{X} = \text{Ca}$ ,  $\text{Sr}$  and  $\text{Ba}$ ) exploration under high pressure. We found that  $\text{SrN}_6$  has a new  $P\bar{1}$  phase at a pressure of 22 GPa and an infinite nitrogen chain structure, and  $\text{BaN}_6$  has a new  $C2/m$  phase at 110 GPa, with an  $\text{N}_6$  ring network structure. Further, we observed that the infinite nitrogen chain and the  $\text{N}_6$  ring network structure contain typical covalent bonds formed by the hybridization of the  $\text{sp}^2$  and  $\text{sp}^3$  orbitals of N, respectively. It is found that both  $\text{SrN}_6$  and  $\text{BaN}_6$  are semiconductor materials and the N-2p orbital plays an important role in the stability of the crystal structure for  $P\bar{1}$ - $\text{SrN}_6$  and  $C2/m$ - $\text{BaN}_6$ . Because of the polymerization of nitrogen in the two compounds and their stabilities under high pressure, they can be used as potential high energy-density materials. The research in this paper further promotes the understanding of alkaline earth metal N-rich compounds and provides new information and methods for the synthesis of alkaline earth metal N-rich compounds ( $\text{XN}_6$ ,  $\text{X} = \text{Ca}$ ,  $\text{Sr}$  and  $\text{Ba}$ ).

Received 2nd March 2021  
Accepted 3rd May 2021

DOI: 10.1039/d1ra01631h

rsc.li/rsc-advances

## 1 Introduction

The nitrogen molecule has a strong triple bond and high bond energy, and it is difficult to react under environmental conditions.<sup>1</sup> Polynitrogen compounds and polymer nitrogen are favored because of their excellent energy density, energy storage characteristics,<sup>2</sup> unique chemical character, and thermodynamic stability.<sup>3</sup> As is known, there are significant energy differences between the nitrogen–nitrogen single bond ( $160 \text{ kJ mol}^{-1}$ ), nitrogen–nitrogen double bond ( $418 \text{ kJ mol}^{-1}$ ), and nitrogen–nitrogen triple bond ( $954 \text{ kJ mol}^{-1}$ ). When multi-nitrogen compounds containing single bonds and double bonds are converted into nitrogen molecules, the bonding method between nitrogen and nitrogen changes, which will release a lot of energy.<sup>4</sup>

High energy-density materials (HEDMs) are generally based on the energy density of HMX ( $5.7 \text{ kJ g}^{-1}$ ).<sup>5</sup> High energy-density materials usually refer to high-energy explosives.<sup>3</sup> Generally, an ideal HEDM should have the following characteristics: (i) high density, (ii) positive heat of formation, (iii) high detonation

performance, (iv) low sensitivity towards external stimuli, (v) good thermal stability. In previous studies, for instance, scientists successfully synthesized cubic gauche nitrogen ( $cg\text{-N}$ )<sup>6</sup> containing only single bonds under the condition of (110 GPa, 2000 K),<sup>7,8</sup> it can be used as a potential high energy-density material. Therefore, N-rich compounds containing a large amount of nitrogen and nitrogen single bond and double bonds may become potential high energy-density materials. Above the stability field of  $cg\text{-N}$ , a layered polymer (LP)<sup>9</sup> with a similar  $Pba2$  phase<sup>10</sup> between 120–180 GPa and a hexagonal layered polynitrogen phase<sup>10</sup> with a pressure around 250 GPa were also synthesized. In order to stabilize the polynitrogen compounds<sup>11</sup> as well as reduce the pressure and conditions for their synthesis, recently, an effective way is to add a small amount of metal atoms to pure nitrogen system through high pressure technology to stabilize the single and double bonds structure to form N-rich compounds.<sup>12</sup> Using this research method, scientists have obtained a large number of N-rich metal compounds, for example, alkali metal and alkaline earth metal N-rich compounds.<sup>13,14</sup> Metal atoms will cause the redistribution of electrons, leading to changes in chemical bonds, which can reduce the pressure of synthesis and increase energy storage.<sup>14</sup>

The high pressure compression to form novel compounds has become a valuable method,<sup>15,16</sup> and the advantage is that it is easy to control and can help obtain more structures of N-rich

School of Physics and Optoelectronic Engineering, Shandong University of Technology, 250049 Zibo, China. E-mail: weishuli@sdu.edu.cn; sunyuping@sdu.edu.cn

† Electronic supplementary information (ESI) available. See DOI: 10.1039/d1ra01631h



nitrides to form stable polynitrogen. High pressure can change the bonding mode, leading to different bond lengths and hybridization modes, forming a rich multi-center covalent polymerization landscape.<sup>4</sup> The change in the crystal structure caused by pressure has been proved by predicting the structural diversity of metal nitrides: N<sub>3</sub>,<sup>15</sup> N<sub>4</sub>,<sup>17</sup> N<sub>5</sub>,<sup>18</sup> cyclo-N<sub>6</sub>,<sup>17</sup> N<sub>8</sub>,<sup>19</sup> N<sub>10</sub>,<sup>20</sup> infinite nitrogen chain<sup>21</sup> and nitrogen network structure,<sup>22</sup> which provide an effective way to obtain N-rich compounds. In recent years, alkaline earth metal N-rich compounds have been theoretically predicted with important research significance as high energy-density materials under high pressure. Compared with alkali metals (Li,<sup>23</sup> K,<sup>24</sup> Na,<sup>25</sup> Rb<sup>26</sup> and Cs<sup>27</sup>), alkaline earth metals (Mg,<sup>17</sup> Be,<sup>28</sup> Ca,<sup>19</sup> Sr<sup>29</sup> and Ba<sup>30</sup>) and transition metals (Sc,<sup>31</sup> Fe,<sup>32</sup> Zn,<sup>33</sup> Ag<sup>34</sup> and Ir<sup>35</sup>) has more valence electrons than alkali metals, which are easier to improve the diversity of polymerized nitrogen forms. We have summarized the pressure ranges that exist the stable structures of alkali metals, alkaline earth metals and transition metals, in the Table S1 in ESI.† We also explained the reason for the transition pressure to decrease for the formation of polymeric nitrogen when we move from ionic azide to covalent azide, in the ESI.†

In this paper, we have predicted the stable phase structures of XN<sub>6</sub> (Sr, Ba) alkaline earth metal N-rich compounds, analyzed the phase stability, and further studied their potential applications as high energy-density materials.<sup>3</sup> The theoretical prediction found that the new phase of *P* $\bar{1}$ -CaN<sub>6</sub> is unstable under high pressure, while the new phase of *P* $\bar{1}$ -SrN<sub>6</sub> is metastable under pressure, and *C2/m*-BaN<sub>6</sub> has been reported to be a metastable phase.<sup>30</sup> In this paper, the *P* $\bar{1}$ -SrN<sub>6</sub> at 22 GPa and *C2/m*-BaN<sub>6</sub> at 110 GPa were predicted to be stable under the corresponding high pressure conditions. After theoretical prediction and calculation, we found that the infinite nitrogen chain structure in the *P* $\bar{1}$ -SrN<sub>6</sub> structure is formed by polymerization when the *Fddd*-SrN<sub>6</sub> structure is under pressure of 22 GPa. And the six-membered annular network structure in the *C2/m*-BaN<sub>6</sub> structure is formed by polymerization when the *Fmmm*-BaN<sub>6</sub> structure is under pressure of 110 GPa. We calculated the electronic band structure and projected density of states for SrN<sub>6</sub> and BaN<sub>6</sub>, and they are all semiconductor materials. By Zintl-Klemm theory<sup>36</sup> and calculating the electronic localization function,<sup>37</sup> we know that the bonding manner of nitrogen atoms for *P* $\bar{1}$ -SrN<sub>6</sub> in high pressure is nitrogen–nitrogen single bond and double bonds and *C2/m*-BaN<sub>6</sub> in high pressure the bonding manner of nitrogen atoms is nitrogen–nitrogen single bond. Due to their content of a large number of nitrogen–nitrogen single bond and double bonds, they can be used as a potential high energy-density material. The research in this paper provides new perspective for the exploration of XN<sub>6</sub> system in the future.

## 2 Computation details

In order to find the stable structures of XN<sub>6</sub> (X = Ca, Sr and Ba) alkaline earth metal N-rich compounds in the pressure range of 0–200 GPa, we used the CALYPSO<sup>38</sup> structure prediction method based on swarm intelligence.<sup>39,40</sup> We selected a point every 10 GPa in the pressure range of 0–200 GPa, and performed high

pressure theoretical predictions and optimization on XN<sub>6</sub> (X = Ca, Sr, Ba) alkaline earth metal N-rich compounds. The CALYPSO structure prediction method has been successfully applied to various systems from elementary solids to binary and ternary compounds.<sup>41</sup> The optimization of the structure and the calculation of the electronic structure is performed within the framework of density functional theory (DFT),<sup>42</sup> implemented by the VASP (Vienna *Ab initio* Calculation Simulation Package) code,<sup>43</sup> and the (GGA) generalized gradient approximation<sup>44</sup> PBE functional is used for calculation. The projector-augmented wave (PAW)<sup>45</sup> method and the Sr, Ba and N potentials were adopted from the VASP potential library, and 5s<sup>2</sup>, 6s<sup>2</sup> and 2s<sup>2</sup> 2p<sup>3</sup> were treated as valence electrons for Sr, Ba and N atoms to calculate the electron–ion interaction. A plane-wave basis set cutoff of 800 eV, a Monkhorst–Pack *k* mesh spacing of  $2\pi \times 0.03 \text{ \AA}^{-1}$  in the Brillouin zone<sup>46</sup> was selected to ensure that all enthalpy calculations converged to less than 1 meV per atom. The relative thermodynamic stability of different XN<sub>6</sub> (X = Ca, Sr and Ba) alkaline earth metal N-rich compounds is calculated as follows:

$$\Delta H (\text{XN}_6) = [H (\text{XN}_6) - H (\text{X}) - 6H (\text{N}_2)/2]/(1 + 6)$$

(X = Ca, Sr and Ba). Select to elemental solid X (X = Ca, Sr and Ba), solid calcium (*fcc*, *bcc*, and  $\beta$ -tin phases), solid strontium (*bcc*, *hcp*, *P6<sub>3</sub>/mmc*), solid barium (*bcc*, *Im3m*, *hcp*, *P6<sub>3</sub>/mmc*) and solid nitrogen  $\alpha$ , *Pbcn*, *P2/c*, *P4<sub>1</sub>2<sub>1</sub>2*, *I2<sub>1</sub>3*, *Pba2*, and *cg*-N phases were used as reference structures in their corresponding stable pressure ranges.  $H = U + PV$  is the enthalpy value of each component,  $\Delta H$  is the enthalpy of formation of each compound, and the *U*, *P* and *V* are thermodynamic energy, pressure and volume respectively. The crystal structure image is made using VESTA software.<sup>47</sup> The dynamical stability of the predicted structure is determined by phonon calculations using a supercell approach with the finite displacement method as implemented in the Phonopy code.<sup>48,49</sup>

## 3 Results and discussions

In recent studies, we have found that metal nitrides have attracted more and more attention.<sup>50,51</sup> Because metal nitrides are more stable than pure nitrogen compounds in terms of kinetics, and have the characteristics of low synthesis pressure and superior physical and chemical properties, they can be widely used in the research of high energy-density materials.<sup>3</sup>

### 3.1 CaN<sub>6</sub> with *P* $\bar{1}$ structure

Since the Ca element is adjacent to the K element and can provide one more electron than the K element, this is more conducive to the diversity of nitrogen forms under high pressure. In previous studies, KN<sub>3</sub> has been successfully predicted theoretically and can be used as a potential high energy-density material.<sup>52</sup> This section mainly studies the structural properties and stability of CaN<sub>6</sub>, we found that a new transition phase of CaN<sub>6</sub> occurred, and the *Fddd* structure under normal pressure was changed to the *P* $\bar{1}$  structure at 32 GPa up to 100 GPa, as shown in Fig. 1(a). The infinite nitrogen chain structure in the



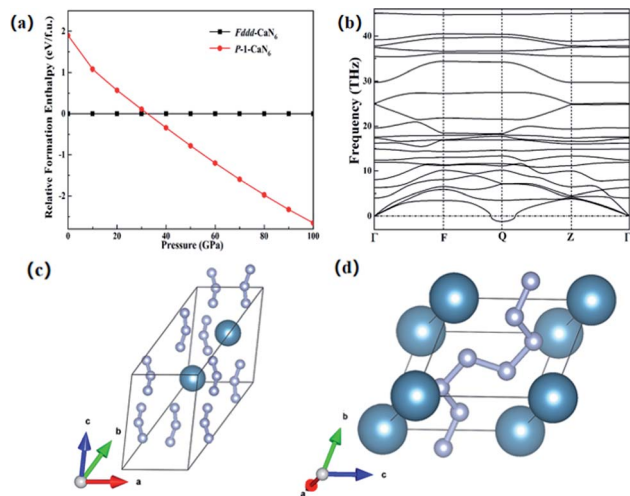


Fig. 1 (a) Relative formation enthalpy of  $P\bar{1}$ - $\text{CaN}_6$  structure and  $Fddd$ - $\text{CaN}_6$  structure under different pressures. (b) The phonon spectrum of  $P\bar{1}$ - $\text{CaN}_6$  structure. (c) Schematic diagram of the  $\text{CaN}_6$  crystal structure under normal pressure. (d) Schematic diagram of the  $P\bar{1}$ - $\text{CaN}_6$  crystal structure under high pressure, the large blue balls represent Ca atoms, and the small balls represent nitrogen atoms.

$P\bar{1}$ - $\text{CaN}_6$  structure is composed of multiple nitrogen atoms, and its structural feature is an infinite armchair-shaped nitrogen chain,<sup>53</sup> as shown in Fig. 1(d). It is polymerized by  $Fddd$ - $\text{CaN}_6$  structure under 32 GPa, and  $Fddd$ - $\text{CaN}_6$  structure was shown in Fig. 1(c).

Referring to previous theoretical studies, we generally consider that the length of a single (N–N) bond is 1.45 Å, a double bond (N=N) equals 1.25 Å,<sup>18</sup> and the length of a triple bond (N≡N) is 1.10 Å at ambient conditions.<sup>33</sup> The bond length between nitrogen and nitrogen in  $P\bar{1}$ - $\text{CaN}_6$  is between 1.23 Å and 1.35 Å, surviving in the alternating range of single and double bonds. In  $P\bar{1}$ - $\text{CaN}_6$  structure, the smallest unit formed by six nitrogen atoms can be equivalent to  $\text{N}_6^{2-}$  anion, this is caused by the calcium atom transfers two valence electrons into the  $\text{N}_6$  structure, showing in the form of  $\text{Ca}^{2+}(\text{N}_6)^{2-}$ . In  $\text{N}_6^{2-}$  unit, the nitrogen atom satisfies the Zintl-Klemm theory,<sup>36</sup> the covalent bonds are formed between the adjacent nitrogen atom,

and form nitrogen–nitrogen single bond and nitrogen–nitrogen double bonds coexistence status. In  $P\bar{1}$ - $\text{CaN}_6$ , the weight ratio of nitrogen is about 67%, due to the presence of single bond and double bonds of nitrogen and nitrogen, when it generates  $\text{N}_2$ , it will release a lot of energy, which can theoretically be used as a potential high energy-density material. We further analyzed the dynamic stability of the  $P\bar{1}$ - $\text{CaN}_6$  structure, and obtained the phonon dispersion curves after calculation, as shown in Fig. 1(b). It can be seen that imaginary frequencies appear in the entire Brillouin zone, indicating the  $P\bar{1}$ - $\text{CaN}_6$  structure are not kinetically stable, so the  $P\bar{1}$ - $\text{CaN}_6$  does not stable structure. However, our analysis of  $\text{N}_6^{2-}$  anion has provided valuable information for the study of other metal polynitrides.

### 3.2 $\text{SrN}_6$ with $P\bar{1}$ structure

This section mainly studies the structural properties and stability of  $\text{SrN}_6$ , and other forms of strontium nitrogen compounds  $\text{SrN}_n$  ( $n = 1-6$ ) have been reported.<sup>51</sup> In previous theoretical prediction, many alkali metal nitrides have been studied and proved to be good energy storage materials, such as  $\text{RbN}_3$ .<sup>26</sup> Because Sr element is adjacent to Rb element, Rb and its compounds have excellent physical and chemical properties such as easy ionization, radiation resistance, energy storage, etc., and are used in various fields.<sup>54</sup> Because  $\text{RbN}_3$  contains nitrogen–nitrogen double bonds and exists stably, it can be used as a potential high energy-density material, that makes strontium nitrogen compound important research significance.<sup>55</sup> After theoretical prediction and calculation, we found that the  $Fddd$ - $\text{SrN}_6$  structure under ambient pressure can be transformed into a  $P\bar{1}$ - $\text{SrN}_6$  structure at 22 GPa, and a new polymerization phase of N occurred, as shown in Fig. 2(a). The  $Fddd$ - $\text{SrN}_6$  structure contains an independent unit consisting of every three nitrogen atoms, as shown in Fig. 2(b), and the infinite nitrogen chain structure in the  $P\bar{1}$ - $\text{SrN}_6$  structure is formed by polymerization when the  $Fddd$ - $\text{SrN}_6$  structure is under pressure of 22 GPa, as shown in Fig. 2(c). The structural parameter information of  $P\bar{1}$ - $\text{SrN}_6$  is shown in Table 1.

We further studied the dynamic stability of  $P\bar{1}$ - $\text{SrN}_6$  structure, and we obtained the phonon dispersion curves of  $P\bar{1}$ - $\text{SrN}_6$

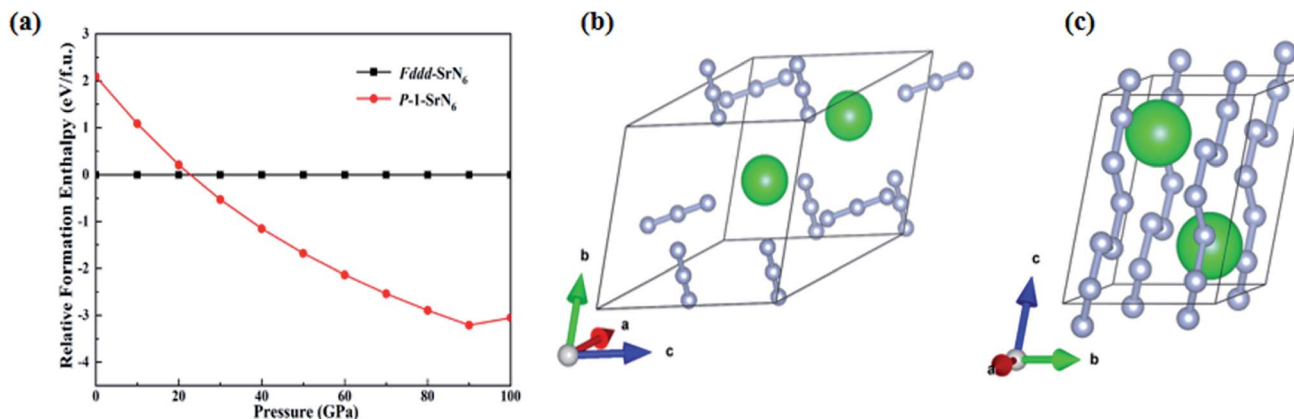


Fig. 2 (a) Relative formation enthalpy of the high-pressure phase  $P\bar{1}$ - $\text{SrN}_6$  structure relative to the normal pressure phase  $Fddd$ - $\text{SrN}_6$  structure under different pressures. (b) Schematic diagram of  $Fddd$ - $\text{SrN}_6$  structure. (c) Schematic diagram of  $P\bar{1}$ - $\text{SrN}_6$  structure. The large green balls are Sr atoms and the small balls are nitrogen atoms.



Table 1 The predicted structural parameters of SrN<sub>6</sub> and BaN<sub>6</sub> under phase change pressure

Phase	<i>P</i> (GPa)	<i>Z</i>	Space group	Lattice parameters (Å, °)	N–N distance/average (Å)	Atomic coordinates (fractional)
SrN <sub>6</sub>	22	2	<i>P</i> $\bar{1}$	<i>a</i> = 5.28 <i>b</i> = 5.29 <i>c</i> = 5.57 $\alpha$ = 91.85 $\beta$ = 112.27 $\gamma$ = 62.78	1.32	Sr (0.608, 0.294, 0.780) N (0.179, 0.210, 0.690) (0.735, 0.741, 0.687) (0.130, 0.197, 0.904) (0.944, 0.247, 0.479) (0.684, 0.743, 0.900) (0.008, 0.748, 0.736)
BaN <sub>6</sub>	110	2	<i>C</i> 2/ <i>m</i>	<i>a</i> = 4.43 <i>b</i> = 4.78 <i>c</i> = 6.25 $\alpha$ = 90.00 $\beta$ = 121.04 $\gamma$ = 90.00	1.38	Ba (0.500, −0.500, 0.500) N (1.196, −0.500, 0.774) (1.818, −0.763, 0.917)

structure. It can be seen from the Fig. 3(a) that no virtual frequency appears in the entire Brillouin zone, indicating that *P* $\bar{1}$ -SrN<sub>6</sub> structure is dynamically stable. The infinite nitrogen chain structure is joined together by covalent bonds, and the valence electrons of Sr atoms are transferred to the N atoms, which plays a very important role in its stability. We calculated the electronic band structure and projected density of states for SrN<sub>6</sub>, and found that SrN<sub>6</sub> is a semiconductor material, as shown in Fig. 3(b) and (c). In the projected density of states diagram, we can observe that the 2p state of N occupies a large proportion of the entire energy range, indicating that the valence electron state of N-2p also plays an important role in the stability of the *P* $\bar{1}$ -SrN<sub>6</sub> crystal structure, as shown in Fig. 3(c). As we all know, the polymerized form of nitrogen plays an important role in high energy-density material. In the infinite nitrogen chain of the *P* $\bar{1}$ -SrN<sub>6</sub> structure, every six nitrogen atoms form a unit and combine with one Sr atom. Since the Sr atom loses two electrons to form a Sr<sup>2+</sup> cation, the nitrogen atoms in each unit get electrons combine with Sr atom. In a unit formed

by every six nitrogen atoms, the nitrogen atom satisfies the Zintl–Klemm theory,<sup>36</sup> which makes the nitrogen atom produce bond with the surrounding atoms, showing in the form of Sr<sup>2+</sup>(N<sub>6</sub>)<sup>2−</sup>, so the nitrogen and the nitrogen form nitrogen–nitrogen single bond and nitrogen–nitrogen double bonds coexistence status. Due to the existence of nitrogen–nitrogen single bond and nitrogen–nitrogen double bonds in the *P* $\bar{1}$ -SrN<sub>6</sub> structure and the nitrogen content reaches 49%, so it is easy to form polymeric nitrogen and conducive to obtaining high energy-density material.

In order to confirm this conclusion and gain a deeper understanding of the microscopic bonding mechanism of SrN<sub>6</sub>, we calculated the electronic localization function diagram and found that the nitrogen atoms have strong electronic localization and form typical covalent bonds, as shown in Fig. 3(d). The electronic local function is a three-dimensional spatial function used to characterize the distribution of electronic positioning, and its value is 0 to 1. When ELF = 1, it means the electrons are completely localized, and when ELF = 0, it means the electrons are completely delocalized, and when ELF = 0.5, it means that electrons are free. The ELF can explain the bonding and electronic distribution between the atoms, and can further explain microscopic bonding mechanisms. In Fig. 3(d), the nitrogen atoms form a chained structure, and they participate in bond formation in the form of sp<sup>2</sup> hybridization. The two sp<sup>2</sup> hybrid orbitals of all nitrogen atoms form covalent bond with one sp<sup>2</sup> hybrid orbital of two adjacent nitrogen atoms. The remaining one sp<sup>2</sup> hybrid orbitals are filled with isolated electrons. In the [−N<sub>6</sub><sup>2−</sup>], due to the sp<sup>2</sup> hybridization of the nitrogen atom, there are nitrogen–nitrogen single bonds and nitrogen–nitrogen double bonds between nitrogen and nitrogen.<sup>33</sup> After calculation, in the infinite nitrogen chain, the distance between nitrogen and nitrogen is between 1.28 Å and 1.38 Å, there is surviving in the alternating range of single and double bonds. It is further proved that the structure of *P* $\bar{1}$ -SrN<sub>6</sub> contains nitrogen–nitrogen single bond and nitrogen–nitrogen double bonds. In the previously reported article, the N-rich compounds with the infinite nitrogen chain structures have high energy density, in the ESI.† In the above analysis, we can judge that the content of nitrogen–nitrogen single bond and double bonds in

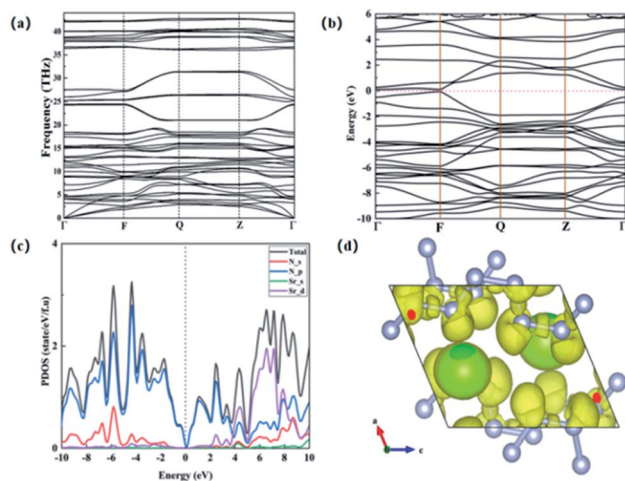


Fig. 3 (a) The phonon spectrum of *P* $\bar{1}$ -SrN<sub>6</sub> structure. (b) Calculated electronic band structure diagram. (c) The calculated projected density of states (PDOS) at 22 GPa. (d) SrN<sub>6</sub> electronic local function graph.



$P\bar{1}$ - $\text{SrN}_6$  is relatively high, which a large amount of energy will be released when  $\text{N}_2$  is generated, and the synthesis pressure is low, so  $P\bar{1}$ - $\text{SrN}_6$  can theoretically be used as a potential high energy-density material.

### 3.3 $\text{BaN}_6$ with $C2/m$ structure

Recently, the latest research on alkaline earth metal nitrides found that Ba and N can form a variety of compounds under high pressure.<sup>30</sup> In this section, we mainly studied the crystal structure properties of the N-rich alkaline earth metal compound  $\text{BaN}_6$ . In previous theoretical predictions, the alkaline earth metal N-rich compounds formed by alkaline earth metals Be,<sup>28</sup> Mg,<sup>17</sup> Ca<sup>19</sup> and non-metallic N elements can be used as potential high energy-density materials. The chemical properties of Ba element are very active and can react with most non-metals, such as  $\text{O}_2$ ,  $\text{N}_2$ ,  $\text{H}_2$ , etc. Ba element has strong reducibility and can form +2 cations, which is easy to combine with the N element under high pressure, so that the Ba element can better promote the diversity of poly-nitrogen forms.<sup>36</sup> Therefore, exploring the alkaline earth metal N-rich compound  $\text{BaN}_6$  as a potential high energy-density material has important research significance.

After theoretical calculations, the relative formation enthalpies of the five structures of  $\text{BaN}_6$  are obtained under different pressures, as shown in Fig. 4(a). After theoretical prediction, it is found that there is a  $P\bar{1}$ (I)- $\text{BaN}_6$  structure with the lowest enthalpy value in the range of 21–110 GPa. This indicates that the  $Fm\bar{3}m$ - $\text{BaN}_6$  structure can be transformed to  $P\bar{1}$ (I)- $\text{BaN}_6$  structure at  $P = 21$  GPa. Our prediction of the  $P\bar{1}$ (I)- $\text{BaN}_6$  structure is consistent with the previous predictions of Huang *et al.*,<sup>30</sup> which also shows that our high-pressure theoretical predictions and calculation results are accurate. Further by theoretically prediction to high-pressure 200 GPa, it is found that a new monoclinic transition phase appears under the

pressure of 110 GPa, the  $C2/m$ - $\text{BaN}_6$  structure, as shown in Fig. 4(c). This indicates that the  $Fm\bar{3}m$ - $\text{BaN}_6$  structure can be transformed to  $C2/m$ - $\text{BaN}_6$  structure at  $P = 110$  GPa. The nitrogen atoms in the  $Fm\bar{3}m$ - $\text{BaN}_6$  structure exists as an independent unit for every two nitrogen atoms, as shown in Fig. 4(b). In the  $P\bar{1}$ (I)- $\text{BaN}_6$  structure, under the pressure of 21 GPa, the polymerization form of nitrogen is formed by the polymerization of nitrogen five-rings and one nitrogen atom, as shown in Fig. 4(d). Under the pressure of 110 GPa, the nitrogen atoms polymerize to form the  $\text{N}_6$  ring network structure<sup>22</sup> in  $C2/m$ - $\text{BaN}_6$ , as shown in Fig. 4(c). It can be seen from the crystal structure diagram that with the increase of pressure, the degree of polymerization of nitrogen in the three structures gradually increases, indicating that pressure can cause the polymerization of nitrogen to form nitrogen polymers. Here, we mainly calculated and analyzed the performance of  $C2/m$ - $\text{BaN}_6$  structure. The structure parameter information of  $C2/m$ - $\text{BaN}_6$  is given in Table 1.

We further studied the dynamic stability of  $C2/m$ - $\text{BaN}_6$  structure, and obtained the phonon dispersion curves by theoretical calculations, and found that there was no imaginary frequency phenomenon in the entire Brillouin zone, indicating that  $C2/m$ - $\text{BaN}_6$  structure it is dynamically stable, as shown in Fig. 5(a). Previous studies have shown that the monoclinic  $C2/m$ - $\text{BaN}_6$  structure exists in the form of metastable state.<sup>30</sup> In order to analyze the electronic properties of  $C2/m$ - $\text{BaN}_6$ , so we calculated the electronic band structure and projected density of states for  $\text{BaN}_6$  and we found that  $\text{BaN}_6$  is a semiconductor material, as shown in Fig. 5(b) and (c). Because Ba element has a higher ionization energy, it is easy to combine with N element, so that valence electrons can be easily transferred to the  $\text{N}_6$  ring network structure. In Fig. 5(c), it can be seen that the N-2p orbital occupies a large proportion of the entire energy map, which indicates that the N-2p orbital plays an important role in

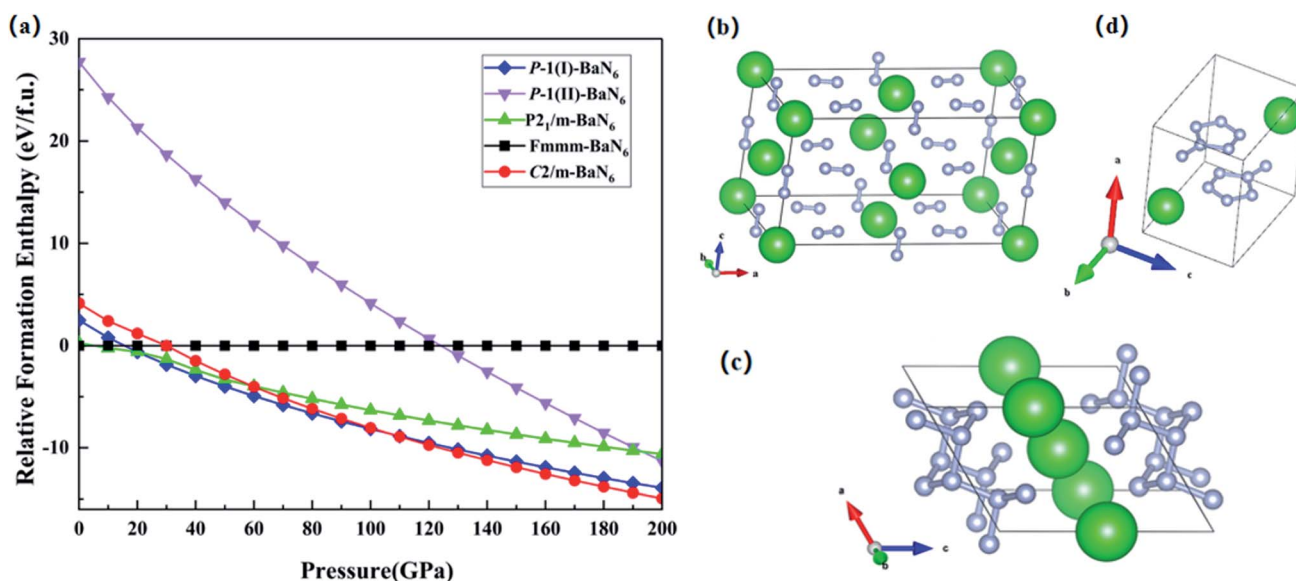


Fig. 4 (a) The relative enthalpy of formation of  $\text{BaN}_6$  with five structures under different pressures. (b)  $Fm\bar{3}m$ - $\text{BaN}_6$  crystal structure diagram. (c)  $C2/m$ - $\text{BaN}_6$  crystal structure diagram. (d)  $P\bar{1}$ (I)- $\text{BaN}_6$  crystal structure diagram. The large green balls are Ba atoms, and the small balls are nitrogen atom.



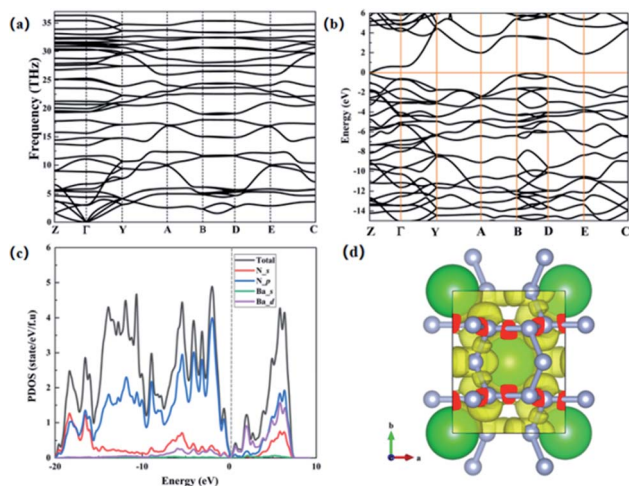


Fig. 5 (a) The phonon spectrum of  $C2/m$ - $BaN_6$  structure. (b) Calculated electronic band structure diagram. (c) The calculated projected density of states (PDOS) at 110 GPa. (d)  $BaN_6$  electronic local function graph.

maintaining the entire crystal structure, thereby improving the stability of the overall structure and the energy storage content. We calculated the bond length between nitrogen and nitrogen in the  $C2/m$ - $BaN_6$  structure and found that the bond length between nitrogen and nitrogen in the  $N_6$  ring network structure is between 1.37–1.40 Å. Because this values are close to the bond length of the nitrogen–nitrogen single bond,<sup>18</sup> which indicates that the  $N_6$  ring network structure contains a large number of nitrogen and nitrogen single bonds. In the  $C2/m$ - $BaN_6$  structure, the N atom in the  $N_6$  ring satisfies the Zintl–Klemm theory<sup>36</sup> to achieve charge balance. Since the Ba atom loses two electrons becomes +2 valence cations and combined with the  $N_6$  ring networks, the N atoms in the  $N_6$  ring get electrons and combine with Ba showing in the form of  $(Ba_x^{2+}-(N_6)_x^{2-})$ . In addition, in a  $-(N_6)_x^{2-}$ , due to the  $sp^3$  hybridization of the nitrogen atom, each N atom in the  $N_6$  ring forms two or three  $\sigma$  bonds to connect to the surrounding N atoms, so that nitrogen–nitrogen single bond is formed between N and N. Therefore, we can get that the  $C2/m$ - $BaN_6$  structure contains a large number of nitrogen–nitrogen single bonds.

We have carried out theoretical calculations on the microscopic bonding mechanism of the  $C2/m$ - $BaN_6$  structure, as shown in Fig. 5(d). After theoretical calculations, it is found that in the connected  $N_6$  ring network structures there are strong electronic localization and isolated electrons around N atoms. In Fig. 5(d), a nitrogen six-membered ring network structure is formed among nitrogen atoms, and they participate in bond formation in the form of  $sp^3$  hybridization, forming typical covalent bonds. It contains two types of nitrogen atoms, the three  $sp^3$  hybrid orbitals of N1 type atoms form three N–N single bonds with the one  $sp^3$  hybrid orbital of the adjacent three nitrogen atoms. The remaining one  $sp^3$  hybrid orbital is filled with isolated electrons. For every N2 type atom, the two  $sp^3$  hybrid orbitals form two  $\sigma$  bonds with one  $sp^3$  hybrid orbital of the surrounding two nitrogen atoms. Particularly, there are two remaining  $sp^3$  hybrid orbits are not involved in bonding, the

remaining two  $sp^3$  hybrid orbitals are filled with isolated electrons. By analyzing the ELF of  $C2/m$ - $BaN_6$  structure, we can conclude that the degree of N atoms polymerization in  $C2/m$ - $BaN_6$  is relatively higher than other polynitrogen structures, so it has higher energy densities. Therefore, it also can be judged that nitrogen–nitrogen single bond is formed between nitrogen and nitrogen. In the previously reported article, the N-rich compounds with the  $N_6$  ring network structures have high energy density, in the ESI.<sup>†</sup> Since the  $N_6$  ring network structure contains a large number of nitrogen–nitrogen single bonds, and release a large amount of energy when  $N_2$  is generated. Therefore, the  $C2/m$ - $BaN_6$  structure can theoretically be used as a potential high energy-density material.

## 4 Conclusions

This paper mainly studied the pressure-induced stability and polymeric nitrogen in alkaline earth metal N-rich nitrides ( $XN_6$ , X = Ca, Sr and Ba), and the theoretical calculations were carried out by the first principles and CALYPSO theoretical prediction methods. After theoretical calculation,  $P1$ - $SrN_6$  at 22 GPa and  $C2/m$ - $BaN_6$  at 110 GPa were predicted to be stable under the corresponding high pressure conditions. Further theoretical calculations found that the nitrogen in the  $P1$ - $SrN_6$  structure is polymerized in the form of infinite nitrogen chain, and the nitrogen in the monoclinic  $C2/m$ - $BaN_6$  structure is polymerized in the form of an  $N_6$  ring network. Both  $P1$ - $SrN_6$  and  $C2/m$ - $BaN_6$  structures are semiconductor materials. And in the  $P1$ - $SrN_6$  structure, the nitrogen atom is  $sp^2$  hybridized, lead to nitrogen and the nitrogen form nitrogen–nitrogen single bond and nitrogen–nitrogen double bonds coexistence status. In the  $C2/m$ - $BaN_6$  structure, the nitrogen atom is  $sp^3$  hybridized, indicating that the nitrogen atom forms two or three  $\sigma$  bonds with the adjacent nitrogen atom. This electronic structure analysis can theoretically indicate that  $P1$ - $SrN_6$  and  $C2/m$ - $BaN_6$  may be potential high energy-density materials. The research in this article is helpful to understand the potential properties of alkaline earth metal N-rich compounds under high pressure conditions, and provides a new theoretical basis for obtaining high energy-density materials.

## Conflicts of interest

There are no conflicts to declare.

## Acknowledgements

This work was supported by the Natural Science Foundation of Shandong Province (No. ZR2020QA059, ZR2019MA020), Shandong University of Technology Science and Technology PhD Funding.

## References

- 1 C. J. M. van der Ham, M. T. M. Koper and D. G. H. Hetterscheid, *Chem. Soc. Rev.*, 2014, **43**, 5183–5191.
- 2 J. Uddin, V. Barone and G. E. Scuseria, *Mol. Phys.*, 2006, **104**, 745–749.



- 3 T. M. Klapötke, in *High Energy Density Materials*, ed. T. M. Klapötke, Springer Berlin Heidelberg, Berlin, Heidelberg, 2007, pp. 85–121, DOI: 10.1007/430\_2007\_057.
- 4 L. Zhang, Y. Wang, J. Lv and Y. Ma, *Nat. Rev. Mater.*, 2017, **2**, 17005.
- 5 H. Lin, Q. Zhu, C. Huang, D.-D. Yang, N. Lou, S.-G. Zhu and H.-Z. Li, *Struct. Chem.*, 2019, **30**, 2401–2408.
- 6 M. I. Eremets, A. G. Gavriliuk, I. A. Trojan, D. A. Dzivenko and R. Boehler, *Nat. Mater.*, 2004, **3**, 558–563.
- 7 D. Plašienka and R. Martoňák, *J. Chem. Phys.*, 2015, **142**, 094505.
- 8 M. I. Eremets, R. J. Hemley, H.-k. Mao and E. Gregoryanz, *Nature*, 2001, **411**, 170–174.
- 9 D. Tomasino, M. Kim, J. Smith and C.-S. Yoo, *Phys. Rev. Lett.*, 2014, **113**, 205502.
- 10 D. Laniel, G. Geneste, G. Weck, M. Mezouar and P. Loubeyre, *Phys. Rev. Lett.*, 2019, **122**, 066001.
- 11 F. Zahariev, S. V. Dudiy, J. Hooper, F. Zhang and T. K. Woo, *Phys. Rev. Lett.*, 2006, **97**, 155503.
- 12 M. Bykov, S. Chariton, E. Bykova, S. Khandarkhaeva, T. Fedotenko, A. V. Ponomareva, J. Tidholm, F. Tasnádi, I. A. Abrikosov, P. Sedmak, V. Prakapenka, M. Hanfland, H.-P. Liermann, M. Mahmood, A. F. Goncharov, N. Dubrovinskaia and L. Dubrovinsky, *Angew. Chem.*, 2020, **59**, 10666.
- 13 R. J. Bruls, H. T. Hintzen and R. Metselaar, *J. Mater. Sci.*, 1999, **34**, 4519–4531.
- 14 X. Zhang, J. Yang, M. Lu and X. Gong, *RSC Adv.*, 2015, **5**, 21823–21830.
- 15 J. Jiang, P. Zhu, D. Li, Y. Chen, M. Li, X. Wang, B. Liu, Q. Cui and H. Zhu, *J. Phys. Chem. B*, 2016, **120**, 12015–12022.
- 16 C. Ji, F. Zhang, D. Hou, H. Zhu, J. Wu, M.-C. Chyu, V. I. Levitas and Y. Ma, *J. Phys. Chem. Solids*, 2011, **72**, 736–739.
- 17 S. Yu, B. Huang, Q. Zeng, A. R. Oganov, L. Zhang and G. Frapper, *J. Phys. Chem. C*, 2017, **121**, 11037–11046.
- 18 F. Peng, Y. Yao, H. Liu and Y. Ma, *J. Phys. Chem. Lett.*, 2015, **6**, 2363–2366.
- 19 S. Zhu, F. Peng, H. Liu, A. Majumdar, T. Gao and Y. Yao, *Inorg. Chem.*, 2016, **55**, 7550–7555.
- 20 K. Xia, X. Zheng, J. Yuan, C. Liu, H. Gao, Q. Wu and J. Sun, *J. Phys. Chem. C*, 2019, **123**, 10205–10211.
- 21 J. Zhang, A. R. Oganov, X. Li and H. Niu, *Phys. Rev. B*, 2017, **95**, 020103.
- 22 X. Wang, Y. Wang, M. Miao, X. Zhong, J. Lv, T. Cui, J. Li, L. Chen, C. J. Pickard and Y. Ma, *Phys. Rev. Lett.*, 2012, **109**, 175502.
- 23 K. Ramesh Babu, C. Bheema Lingam, S. P. Tewari and G. Vaitheeswaran, *J. Phys. Chem. A*, 2011, **115**, 4521–4529.
- 24 K. Ramesh Babu and G. Vaitheeswaran, *Chem. Phys. Lett.*, 2012, **533**, 35–39.
- 25 M. Zhang, K. Yin, X. Zhang, H. Wang, Q. Li and Z. Wu, *Solid State Commun.*, 2013, **161**, 13–18.
- 26 X. Wang, J. Li, N. Xu, H. Zhu, Z. Hu and L. Chen, *Sci. Rep.*, 2015, **5**, 16677.
- 27 X. Wang, J. Li, H. Zhu, L. Chen and H. Lin, *J. Chem. Phys.*, 2014, **141**, 044717.
- 28 S. Wei, D. Li, Z. Liu, W. Wang, F. Tian, K. Bao, D. Duan, B. Liu and T. Cui, *J. Phys. Chem. C*, 2017, **121**, 9766–9772.
- 29 S. Wei, L. Lian, Y. Liu, D. Li, Z. Liu and T. Cui, *Phys. Chem. Chem. Phys.*, 2020, **22**, 5242–5248.
- 30 B. Huang and G. Frapper, *Chem. Mater.*, 2018, **30**, 7623–7636.
- 31 J. Lin, D. Peng, Q. Wang, J. Li, H. Zhu and X. Wang, *Phys. Chem. Chem. Phys.*, 2021, **23**, 6863–6870.
- 32 L. Wu, R. Tian, B. Wan, H. Liu, N. Gong, P. Chen, T. Shen, Y. Yao, H. Gou and F. Gao, *Chem. Mater.*, 2018, **30**, 8476–8485.
- 33 Z. Liu, D. Li, F. Tian, D. Duan, H. Li and T. Cui, *Inorg. Chem.*, 2020, **59**, 8002–8012.
- 34 N. Yedukondalu, G. Vaitheeswaran, P. Modak and A. K. Verma, *Solid State Commun.*, 2019, **297**, 39–44.
- 35 X. Du, Y. Yao, J. Wang, Q. Yang and G. Yang, *J. Chem. Phys.*, 2021, **154**, 054706.
- 36 F. Wang and G. J. Miller, *Inorg. Chem.*, 2011, **50**, 7625–7636.
- 37 A. D. Becke and K. E. Edgecombe, *J. Chem. Phys.*, 1990, **92**, 5397–5403.
- 38 Y. Wang, J. Lv, L. Zhu and Y. Ma, *Phys. Rev. B: Condens. Matter Mater. Phys.*, 2010, **82**, 094116.
- 39 Y. Wang, J. Lv, L. Zhu and Y. Ma, *Comput. Phys. Commun.*, 2012, **183**, 2063–2070.
- 40 Q. Tong, J. Lv, P. Gao and Y. Wang, *Chin. Phys. B*, 2019, **28**, 106105.
- 41 J. Lv, Y. Wang, L. Zhu and Y. Ma, *Phys. Rev. Lett.*, 2011, **106**, 015503.
- 42 B. Delley, *J. Phys.: Condens. Matter*, 2010, **22**, 384208.
- 43 G. Kresse and J. Furthmüller, *Phys. Rev. B: Condens. Matter Mater. Phys.*, 1996, **54**, 11169–11186.
- 44 J. P. Perdew, K. Burke and M. Ernzerhof, *Phys. Rev. Lett.*, 1996, **77**, 3865–3868.
- 45 X. Blanc, É. Cancès and M.-S. Dupuy, *C. R. Math.*, 2017, **355**, 665–670.
- 46 H. J. Monkhorst and J. D. Pack, *Phys. Rev. B: Solid State*, 1976, **13**, 5188–5192.
- 47 K. Momma and F. Izumi, *J. Appl. Crystallogr.*, 2011, **44**, 1272–1276.
- 48 A. Togo, F. Oba and I. Tanaka, *Phys. Rev. B: Condens. Matter Mater. Phys.*, 2008, **78**, 134106.
- 49 S. D. Dabhi and P. K. Jha, *Polymer*, 2015, **81**, 45–49.
- 50 K. Xia, J. Yuan, X. Zheng, C. Liu, H. Gao, Q. Wu and J. Sun, *J. Phys. Chem. Lett.*, 2019, **10**, 6166–6173.
- 51 B. Advaiah, E. Narsimha Rao and G. Vaitheeswaran, *J. Phys.: Condens. Matter*, 2019, **31**, 475402.
- 52 G. Vaitheeswaran and K. R. Babu, *J. Chem. Sci.*, 2012, **124**, 1391–1398.
- 53 D. Laniel, B. Winkler, E. Koemets, T. Fedotenko, M. Bykov, E. Bykova, L. Dubrovinsky and N. Dubrovinskaia, *Nat. Commun.*, 2019, **10**, 4515.
- 54 W. C. Buttermann and R. G. Reese Jr, *Mineral Commodity Profiles – Rubidium*, Report 2003-45, 2003.
- 55 H. Zhu, X. Han, P. Zhu, X. Wu, Y. Chen, M. Li, X. Li and Q. Cui, *J. Phys. Chem. C*, 2016, **120**, 12423–12428.
- 56 A. A. L. Michalchuk, S. Rudić, C. R. Pulham and C. A. Morrison, *Phys. Chem. Chem. Phys.*, 2018, **20**, 29061–29069.

